energies

MDPI

Article

Relationship between Organic Geochemistry and Reservoir Characteristics of the Wufeng-Longmaxi Formation Shale in Southeastern Chongqing, SW China

Shengxiu Wang [1,2], Jia Wang [3,*], Yuelei Zhang [1,2], Dahua Li [1,2], Weiwei Jiao [2], Jinxi Wang [1], Zhian Lei [4], Zhongqiang Yu [2], Xiaojun Zha [3] and Xianfeng Tan [3,*]

1 National and Local Joint Engineering Research Center of Shale Gas Exploration and Development, Chongqing Institute of Geology and Mineral Resources, Chongqing 401120, China; xiuxiu341@163.com (S.W.); zyl7049@163.com (Y.Z.); ldh@vip.163.com (D.L.); legomeng@163.com (J.W.)
2 Key Laboratory of Shale Gas Exploration, Ministry of Natural Resources, Chongqing Institute of Geology and Mineral Resources, Chongqing 401120, China; Jiaoweiw-210@163.com (W.J.); zhangzhiping4211@163.com (Z.Y.)
3 Chongqing Key Laboratory of Complex Oil and Gas Exploration and Development, Chongqing 401331, China; zzzzzz662021@163.com
4 Chongqing Shale Gas Exploration and Development Company Limited, Chongqing 401121, China; Leiza@petrochina.com.cn
* Correspondence: wangjia@cqust.edu.cn (J.W.); xianfengtan8299@163.com (X.T.)

check for updates

Citation: Wang, S.; Wang, J.; Zhang, Y.; Li, D.; Jiao, W.; Wang, J.; Lei, Z.; Yu, Z.; Zha, X.; Tan, X. Relationship between Organic Geochemistry and Reservoir Characteristics of the Wufeng-Longmaxi Formation Shale in Southeastern Chongqing, SW China. *Energies* **2021**, *14*, 6716. https://doi.org/10.3390/en14206716

Academic Editors: Xixin Wang and Sohrab Zendehboudi

Received: 7 September 2021
Accepted: 30 September 2021
Published: 15 October 2021

Abstract: Shale gas accumulates in reservoirs that have favorable characteristics and associated organic geochemistry. The Wufeng-Longmaxi formation of Well Yucan-6 in Southeast Chongqing, SW China was used as a representative example to analyze the organic geochemical and reservoir characteristics of various shale intervals. Total organic carbon (TOC), vitrinite reflectance (Ro), rock pyrolysis, scanning electron microscopy (SEM), and nitrogen adsorption analyses were conducted, and a vertical coupling variation law was established. Results showed the following: the Wufeng-Longmaxi formation shale contains kerogen types I and II_2; the average TOC value at the bottom of the formation is 3.04% (and the average value overall is 0.78%); the average Ro value is 1.94%; the organic matter is in a post mature thermal evolutionary stage; the shale minerals are mainly quartz and clay; and the pores are mainly intergranular, intragranular dissolved pores, organic matter pores and micro fractures. In addition, the average specific surface area (BET) of the shale is 5.171 m^2/g; micropores account for 4.46% of the total volume; the specific surface area reaches 14.6%; and mesopores and macropores are the main pore spaces. There is a positive correlation between TOC and the quartz content of Wufeng-Longmaxi shale, and porosity is positively correlated with the clay mineral content. It is known that organic pores and the specific area develop more favorably when the clay mineral content is higher because the adsorption capacity is enhanced. In addition, as shale with a high clay mineral content and high TOC content promotes the formation of a large number of nanopores, it has a strong adsorption capacity. Therefore, the most favorable interval for shale gas exploration and development in this well is the shale that has a high TOC content, high clay mineral content, and a suitable quartz content. The findings of this study can help to better identify shale reservoirs and predict the sweet point in shale gas exploration and development.

Keywords: shale gas; nanopores; adsorption capacity; shale intervals; vertical coupling variation law

1. Introduction

With the increasing global demand for energy and diminishing oil and gas resources [1,2], shale gas is a source of clean energy that has become the focus of exploration and development [3–6]. China has achieved shale gas exploration breakthroughs in the south marine strata. Several 100 × 10^9 m^3 shale gas fields have been discovered in Fuling, Changning, Weiyuan, and other areas in southwest China [7–11], and the deepest shale gas exploration

well (well Zu-206) was successfully drilled in China last year. In addition, the daily shale gas production rate in well Lu-203 is 137.9 $\times$ 10^4 m^3, and the cumulative production of shale gas in Fuling shale gas field exceeds 30 $\times$ 10^9 m^3 (People's daily of China, 2019).

Hydrocarbon generation potential and micro reservoirs are two areas of focus in shale gas exploration and geological research [12–14]. Although organic rich shale from the Lower Paleozoic is widely distributed in southern China, there are obvious differences between the geochemical and reservoir characteristics of the shale between different layers and regions. The abundance and maturity of shale organic matter (OM) not only determines its hydrocarbon generation potential but also provides information about its pore structure and adsorption capacity [3,15,16], and this is known to directly affect the natural gas content of the shale and its later development [17–21]. Shale was characterized by typical "self-generation and storage" [3,18], and good organic geochemical indexes and reservoir parameters are the key factors for shale gas rich integrated reservoirs [2,22]. The hydrocarbon generation of organic matter during shale diagenesis will promote the formation of organic matter pores in shale, and the transformation and recrystallization of clay minerals will lead to the changes of shale matrix pores [20,23,24]. Therefore, studying shale geochemistry and its reservoir characteristics is necessary to understand the relationship between the two, and determining this is key to conducting informative shale gas geological research.

Well Yucan-6 is a key parameter well located in southeast Chongqing, and it has indicated good shale gas exploration possibilities to date. In this study, the geology of the area is described. Then, the samples and test methods collected in this study discussed specifically. Finally, Well Yucan-6 was used as a representative example to analyze the geochemical and reservoir characteristic parameters of different shale intervals in the Wufeng formation of the Upper Ordovician-Longmaxi formation of the Lower Silurian. A coupling relationship between shale geochemical characteristics and the physical properties of the reservoir was established, and this in turn revealed the key controlling factors of the differential enrichment of shale gas in this single well. It is anticipated that this study will serve as a research example and provide data support for marine shale gas exploration projects and their associated development in southern China.

2. Geological Setting

The study area is located to the southeast of Chongqing, in southwest China. With respect to the associated geotectonics, the area is situated in the depression structural unit of the Yangtze paraplatform [25,26] and the present structural pattern has undergone superimposition and transformation via the Caledonian, Hercynian, Indosinian, Yanshan, and Xishan tectonic movements. Folds and faults are relatively well developed, and the following fold-thrust belt structural styles are evident from the north west to the south east: partition groove style, transition style, and partition wall style (Figure 1). The main surface outcropping strata to the southeast of Chongqing belong to the Paleozoic followed by the Mesozoic Triassic; a few belong to the Jurassic and Cretaceous. However, tertiary strata are lacking.

The study area mainly comprises deep-water shelf facies from the Late Ordovician to the Early Silurian [27], and the Wufeng-Longmaxi formation shale was deposited accordingly. It has a thickness of 20–109 m, is rich in OM, and is the key stratum series for shale gas exploration and development in southern China. The upper part of the Wufeng-Longmaxi Formation comprises grayish green shale mixed with silty shale or siltstone, the lower part comprises black and dark gray calcareous shale, calcareous silty shale, and graptolite shale, and the bottom comprises black silty carbonaceous shale and siliceous shale. Well Yucan-6 is located to the southeast of the Xiyang Syncline within the barrier fold belt area southeast of Chongqing. The strata are drilled to a depth of 786 m, which reveals 7.71 m of the Wufeng Formation and 76.79 m of the Longmaxi formation.

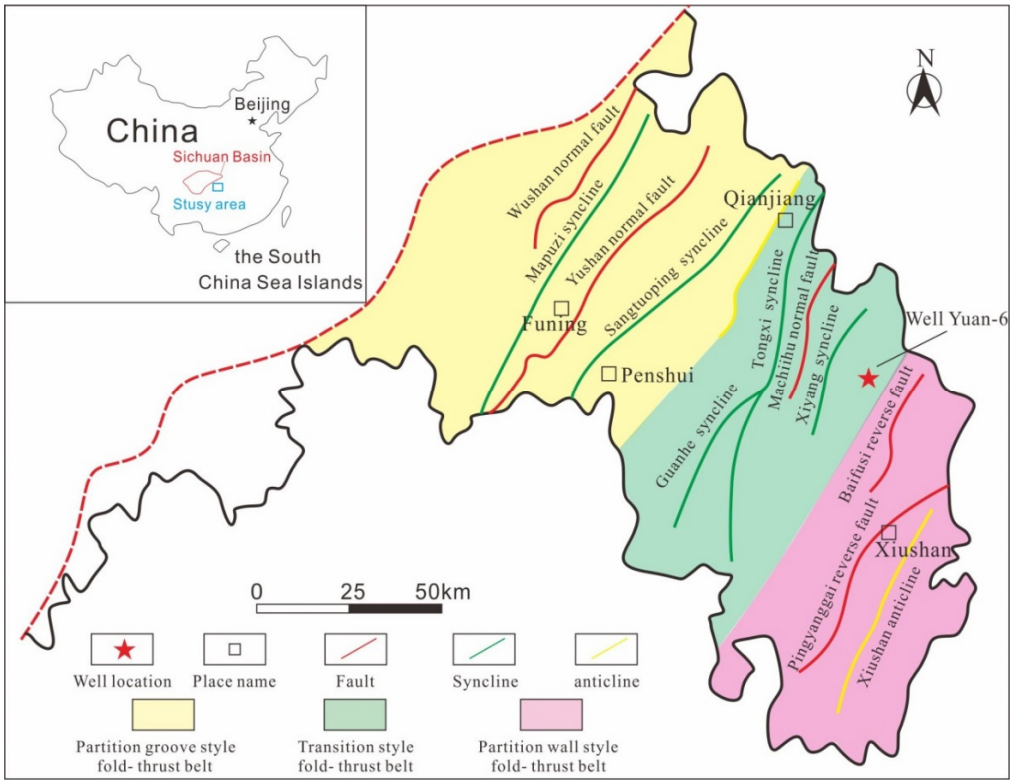

Figure 1. Structural characteristics of study area with location of well Yuan-6.

3. Methods

A dense sampling method was used to obtain 76 shale samples from the shale section of Well Yucan-6. The samples were then crushed to a 200 mesh. Rock-Eval parameters, total organic carbon (TOC), and the pulse porosity and permeability of all samples were respectively obtained using a Rock-Eval VI (RE 6) and a Leco CS-230 carbon and automatic mercury injection instrument (Auto Pore 9500) at the Ministry of Land and Resources of Chongqing Mineral Resources Supervision and Test Center. In addition, the whole rock and clay mineral composition and the reservoir's microscopic characteristics of 17 shale samples (sublevel selected according to the depth of the well from 76 shale samples) were analyzed using X-ray diffraction (XRD) and scanning electron microscopy (SEM); kerogen macerals, kerogen carbon isotopes, specific surface area, rock density, isothermal adsorption properties, and capillary pressure curves of nine shale samples (sublevel selected according to the depth of the well from 17 XRD shale samples) were tested in the State Key Laboratory of Oil and Gas Reservoir Geology and Exploitation at Chengdu University of Technology, China. The sampling and testing of all shale samples wase conducted in strict accordance with shale gas sampling specifications and national standards.

4. Results

The results obtained are presented in the following sub-sections and include the organic geochemical characteristics and the various reservoir characteristics.

4.1. Organic Geochemical Characteristics

Shale in the Wufeng-Longmaxi Formation was developed in a deep-water reduction environment that was conducive for the survival of plankton and the preservation of OM. Shale gas exploration practice has shown that the shale has a good hydrocarbon generating material basis and a good hydrocarbon generation and expulsion process [28,29].

4.1.1. Total Organic Carbon Content

The organic carbon content of Well Yucan-6 shows obvious segmentation characteristics (Figure 2). The TOC values of the Wufeng Formation and the bottom of the Longmaxi Formation are between 1.84% and 4.79%, with an average of 3.04%. However, there is a gradual decrease in the TOC values of the upper shale; values range from 0.159 to 1.52% (with an average of 0.78%), but not many layers exceed 1.0%.

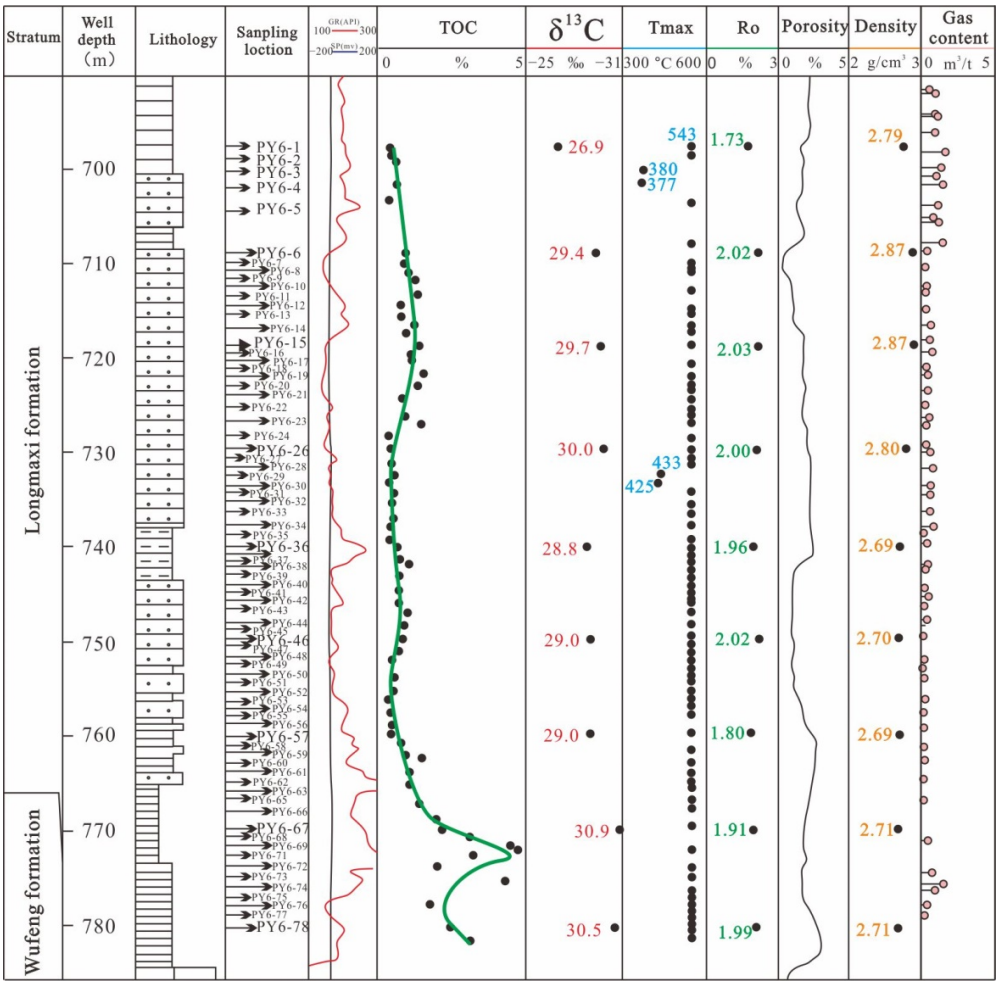

Figure 2. Geochemical parameters at different depths in Well Yucan-6.

4.1.2. Types of Organic Matter (OM)

The kerogen type classification standard of $\delta^{13}C$ proposed by Peters and Cassa [30] is as follows: type I kerogen ranges from −35.0 to −30‰, type II_1 ranges from $-30.0 \leq \delta^{13}C < -27.5$‰, type II_2 ranges from $-27.5 \leq \delta^{13}C < -25$‰ and type III is ≥25.0‰. The kerogen C isotope analysis of the nine shale samples from well Yucan 6 show that the bottom shale of the Wufeng Formation is type I, the upper middle shale is type II_1, and only one sample at the top is type II_2 (Figure 2).

In addition, the formula for the kerogen type index (Ti),

$$\text{Ti} = (\text{sapropelite} \times 100 + \text{Exinite} \times 50 - \text{vitrinite} \times 75 - \text{inertinite} \times 100)/100)$$

provides the following information: the kerogen Ti of type I is greater than 80, that of type II ranges from 0 to 80, and that of type III is less than 0. The results of a maceral analysis of the 17 shale kerogen samples from Well Yucan-6 in the study area showed that all the Ti values were greater than 80 and were thus all type I kerogen (Table 1).

Table 1. Maceral analysis of organic kerogen from Well Yucan-6.

Order Number	Sample Number	Well Depth (m)	Sapropelite (%)	Exinite (%)	Vitrinite (%)	Inertinite (%)	Ti Value	Type
1	YC6-1	697.3	96	0	2	2	92.5	I
2	YC6-4	702.37	96	0	3	1	92.75	I
3	YC6-6	708.71	97	0	2	1	94.5	I
4	YC6-11	710.03	98	0	1	1	96.25	I
5	YC6-15	718.1	97	0	1	2	94.25	I
6	YC6-19	722.53	96	0	3	1	92.75	I
7	YC6-26	729.4	95	0	3	2	90.75	I
8	YC6-31	734.9	98	0	1	1	96.25	I
9	YC6-36	739.8	96	0	1	3	92.25	I
10	YC6-41	744.5	97	0	1	2	94.25	I
11	YC6-46	749.4	96	0	2	2	92.5	I
12	YC6-52	754.9	97	0	2	1	94.5	I
13	YC6-57	759.57	95	0	2	3	90.5	I
14	YC6-62	764.1	96	0	3	1	92.75	I
15	YC6-67	769.5	94	0	3	3	88.75	I
16	YC6-73	775.8	95	0	2	3	90.5	I
17	YC6-78	780.6	97	0	2	1	94.5	I

4.1.3. Maturity of Organic Matter (OM)

According to the asphalt reflectance formula Ro = 0.618Rb + 0.4 [31], the vitrinite reflectance %Ro of Well Yucan-6 ranges from 1.73% to 2.03%, with an average value of 1.94%, and is thus in a post mature stage [30]. The clay mineral diffraction results for the 17 shale samples show that the shale is mainly composed of illite, chlorite, mixed illite-smectite, and mixed chorite-smectite, with mixed layer ratios between 6% and 15% (Table 2). Illite or chlorite appears in the mixed layer at a high content and high order, which is representative of a relatively complete diagenetic evolutionary sequence [32]. These results are consistent with the high Ro value and T_{max} test results that were generally >500 °C, and they show that the shale has reached a hydrocarbon generation peak. However, the results only indicate that the oil generation process has been strong and that crude oil cracking has occurred [26,33]. Therefore, the hydrocarbon generation capacity of the shale is currently limited.

Table 2. X-ray diffraction (XRD) data of shale clay minerals.

Order Number	Sample Number	Well Depth (m)	Clay Mineral Content (%)						Mixed Layer Ratio (% S)	
			K	C	I	S	I/S	C/S	I/S	C/S
1	YC6-1	697.3	/	16	19	/	56	9	6	10
2	YC6-4	702.37	/	11	37	/	46	6	7	12
3	YC6-6	708.71	/	13	33	/	49	5	9	14
4	YC6-11	710.03	/	9	30	/	57	4	7	13
5	YC6-15	718.1	/	10	24	/	58	8	9	11
6	YC6-19	722.53	/	9	28	/	59	4	7	14
7	YC6-26	729.4	/	6	35	/	56	3	8	15
8	YC6-31	734.9	/	6	22	/	68	4	9	12
9	YC6-36	739.8	/	10	20	/	63	7	6	13
10	YC6-41	744.5	/	7	23	/	65	5	7	12
11	YC6-46	749.4	/	8	16	/	69	7	9	11
12	YC6-52	754.9	/	11	15	/	64	10	11	10
13	YC6-57	759.57	/	9	23	/	60	8	10	11

Table 2. *Cont.*

Order Number	Sample Number	Well Depth (m)	Clay Mineral Content (%)						Mixed Layer Ratio (% S)	
			K	C	I	S	I/S	C/S	I/S	C/S
14	YC6-62	764.1	/	8	15	/	70	7	9	9
15	YC6-67	769.5	/	6	20	/	69	5	10	12
16	YC6-73	775.8	/	8	46	/	40	6	7	10
17	YC6-78	780.6	/	10	20	/	63	7	8	11

Notes: K (kaolinite); C (chlorite); I (illite); S (smectite); I/S (mixed illite-smectite); C/S (mixed chlorite-smectite).

4.2. Reservoir Characteristics

The mineral composition, physical characteristics, and pore types of reservoirs were analyzed and are presented in the following.

4.2.1. Mineral Composition

The mineral composition of shale differs depending on its associated sedimentary conditions and the associated diagenetic evolutionary process [32]. The whole rock XRD analysis results show that the Wufeng-Longmaxi formation shale has the following mineral composition and content (see Figure 3 for minerals and percentage contents): a quartz content of between 27.9% and 48.1% (with an average content of 37.82%); a clay mineral content ranging from 14.1 to 50.1% (with average content of 28.84%), which is mainly composed of illite and mixed illite-smectite; a plagioclase content ranging from 4.9% and 20.7% (with an average content of 11.7%); a potash feldspar content ranging from 1.2% and 7.9% (with an average content of 5.07%); a dolomite content ranging from 1.4% and 11.1% (with an average content of 5.86%); and a calcite content ranging from 0.09% to 15.5% (with an average content of 5.62%). In general, the shale mainly comprises quartz and clay minerals, but it is supplemented by feldspar and carbonate minerals and also contains small amounts of pyrite, siderite, and other minerals.

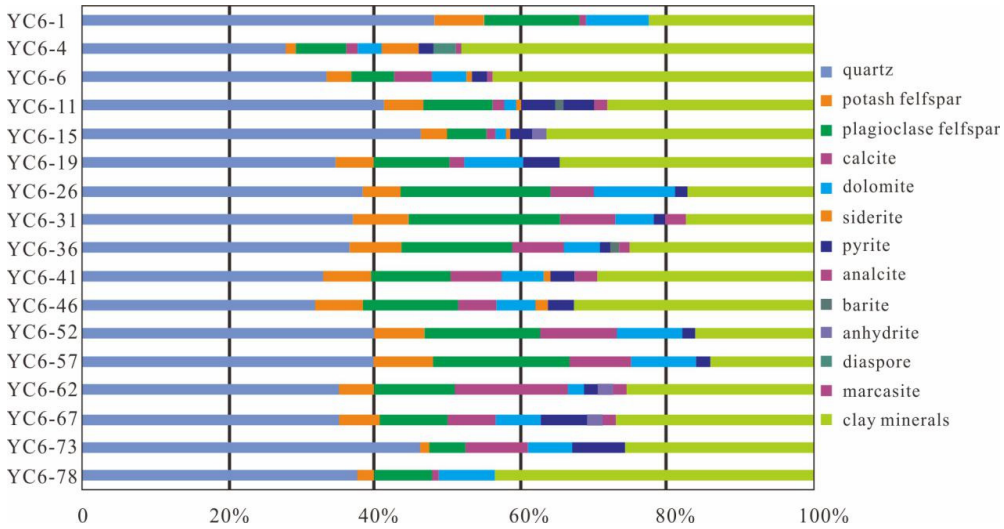

Figure 3. Mineral composition of shale reservoir in Well Yucan-6 (XRD).

4.2.2. Physical Characteristics

The porosity and permeability and the pore structure and associated adsorption capacity were analyzed using various measures and the results are presented in the following.

Porosity and Permeability

Shale generally has a good adsorption capacity, but reservoirs that produce high-yield shale gas often also have high porosity and permeability conditions [34]. Porosity and

permeability measurements of the 76 shale samples showed the following: porosity ranges from 0.11% to 1.32% (with an average of 0.33%) and permeability ranges from 0.0001 to 1.0298 × 10^{-3} μm^2 (with an average value of 0.0279 × 10^{-3} μm^2).

Pore Structure and Adsorption Capacity: High Pressure Mercury Injection

The nine shale samples from Well Yucan-6 were analyzed and tested using high-pressure mercury injection, and the development of pores and their continuity were determined from the mercury injection curves. The curves showed that different mercury injection amounts and displacement pressures were obtained from the various shale samples in Well Yucan-6; however, the curves had similar morphological characteristics and were generally linear with weak segmentation (Figure 4a), and in this respect, they differ from typical high-pressure mercury injection curves [35]. The results were as follows: the separation coefficient (SP) average of the nine samples was 7.27, which indicates that the shale pore distribution range was large. The displacement pressure of the samples was generally low (at less than 10 MPa). The average value of the skewness was 2.90, which is representative of a peak curve with an obvious coarse skewness. The average pore volume measured by the mercury injection method was 0.0078 cm^3/g; the average pore size was large, and most pores measured 0.00–0.025 μm or 2.5–35 μm (Figure 4b). Although the high-pressure mercury injection data are related to clastic samples, and the mercury injection curve is not representative of the true core value, the results nevertheless show that the porosity and permeability conditions and the migration path of the shale would improve after fracture and crushing.

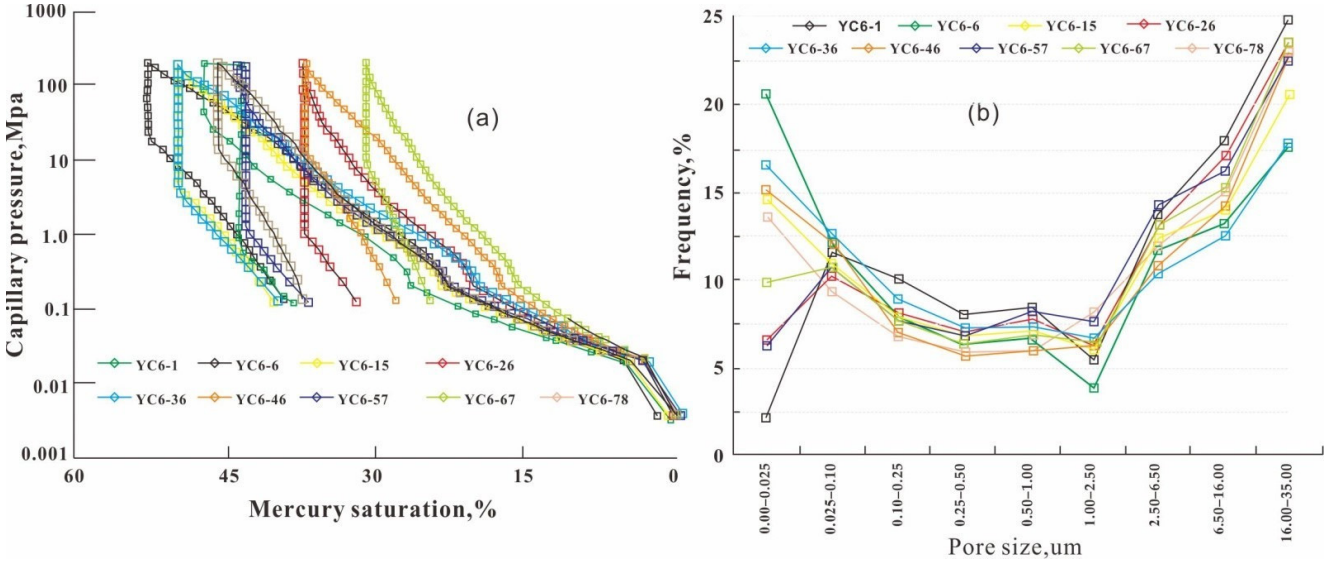

Figure 4. High pressure mercury injection data for shale in Well Yucan-6. (**a**): Capillary pressure curve; (**b**): Pore size distribution.

Pore Structure and Adsorption Capacity: Nitrogen Adsorption

The specific surface area calculated using the Brunauer–Emmett–Telle (BET) method of the nine shale samples from Well Yucan-6 range from 2.0157 m^2/g to 7.155 m^2/g (with an average value of 5.171 m^2/g). The cumulative specific surface area (as determined using the method of Barrett, Joyner and Halenda) (hereafter referred to as BJH) was between 1.17 m^2/g and 2.882 m^2/g (with an average value of 1.965 m^2/g). The total pore volumes calculated using the method of BJH varied from 0.0014 mL/g to 0.0047 mL/g (with an average value of 0.0030 mL/g) (Table 3). The average pore size calculated using the method of BJH was between 4.7591 nm and 8.2132 nm (with an average value of 6.585 nm). According to the division scheme of Sing [36], micropores are defined as measuring < 2 nm, mesoporous as 2–50 nm, and macropores as >50 nm. The data obtained in this study thus

show that these three pore types account for 4.46%, 71.67%, and 23.86% of the total pore volume respectively, and account for 14.60%, 81.11%, and 4.27% of the specific surface area. Although micropores account for 4.46% of the total volume, the specific surface area accounts for 14.6%, which indicates that the shale micropores are relatively well developed and that mesopores and macropores provide the main space and place for shale gas preservation.

Table 3. Experimental nitrogen adsorption data.

Order Number	Sample Number	Specific Surface Area (m^2/g)	Cumulative Specific Surface Area (m^2/g)	Total Pore Volume (mL/g)	Average Pore Size (nm)
1	YC6-1	2.1050	1.170	0.0023	7.7643
2	YC6-6	7.0040	2.882	0.0027	5.4891
3	YC6-15	6.3684	2.107	0.0026	4.8955
4	YC6-26	2.7763	1.303	0.0026	7.8545
5	YC6-36	3.9419	2.076	0.0043	8.2132
6	YC6-46	6.1991	2.736	0.0047	6.8128
7	YC6-57	2.9612	1.390	0.0027	7.8910
8	YC6-67	7.4679	2.813	0.0039	5.5836
9	YC6-78	7.7155	1.215	0.0014	4.7591

The analysis also shows a certain correlation between the specific surface area calculated using the BET method and the total pore volume calculated using the BJH method (Figure 5). When the specific surface area of shale calculated using the BET method was larger, the average pore size was smaller, and when the pore volume calculated using the BJH method was smaller, the average pore size was larger. This shows that micropores not only greatly increase the specific surface area of shale, but that shale can also contain a large number of micropores, which thus reduces the average pore size.

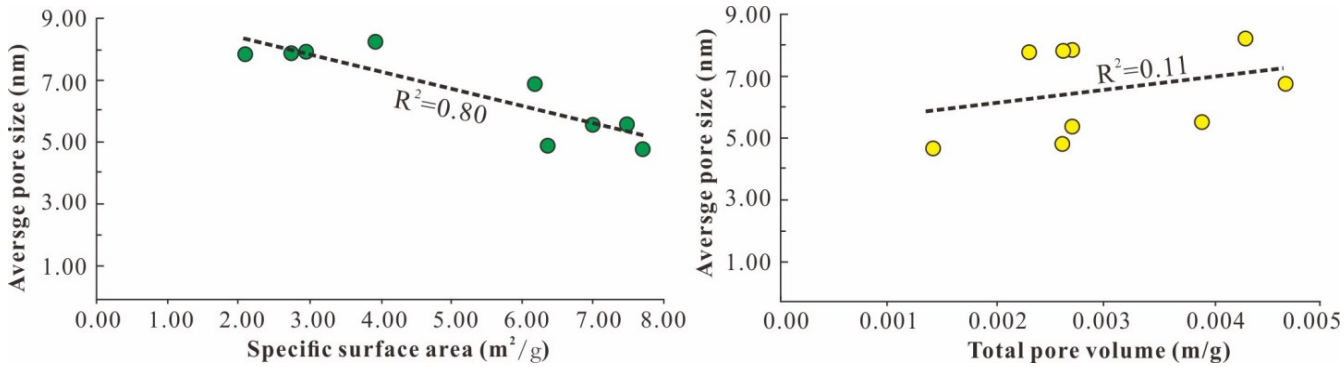

Figure 5. Relationship between specific surface area, total pore volume and pore size of shale.

Pore Structure and Adsorption Capacity: Isothermal Adsorption

An isothermal adsorption experiment was conducted on the nine shale samples. The results showed that the adsorption gas content increased with an increase in pressure. In addition, when the pressure was less than 5 Mpa, the adsorption capacity increased rapidly with an increase in pressure; when the pressure ranged from 5 to 10 Mpa, the growth rate decreased; and with a pressure of more than 10 MPa, the increment in shale adsorption decreased to zero with an increase in pressure until it reached saturation (Figure 6). The Langmuir volume of the nine shale samples ranged from 0.71 to 3.42 m^3/t (with an average value of 1.38 m^3/t), which indicates that the shale has a strong adsorption capacity, and the volume increased in accordance with the depth at which the core sample was obtained. In addition, Langmuir pressure ranged from 1.68 to 2.01 MPa (with an average of 1.83 MPa) (Figure 6). The pressure value was therefore small, which indicates that the adsorption gas

was mainly adsorbed at a low pressure, and there was no obvious incremental adsorption capacity with an increase in pressure.

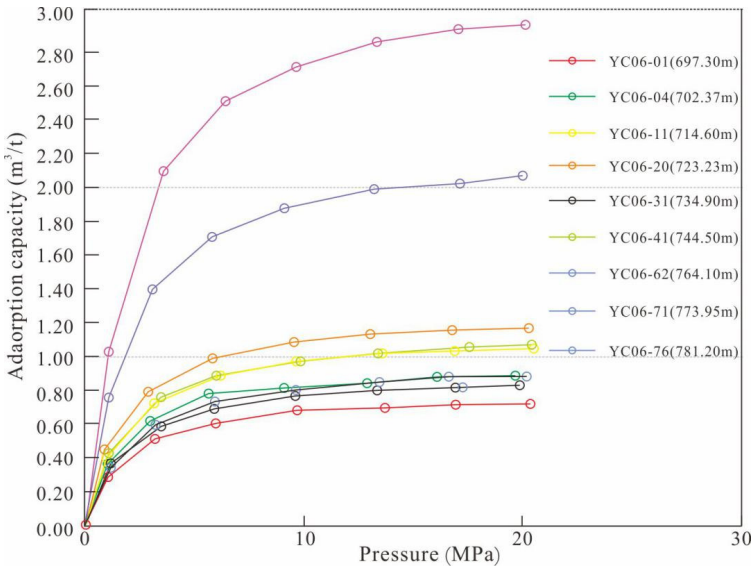

Figure 6. Methane isothermal adsorption curve of shale samples from Well Yucan-6.

4.2.3. Pore Types

To achieve high production, a large capacity shale gas reservoir is required [34]. The organic rich shale of the Wufeng-Longmaxi Formation is dense and it has poor porosity and permeability; however, it contains diverse pore space types and a large number of inorganic pores, organic pores, and micro fractures [3]. These are described as follows:

Inorganic Pores

In conventional reservoirs, large quantities of brittle minerals provide conditions for the development of many intergranular pores, intragranular pores, and dissolution pores [22]. The SEM observations showed the frequent existence of micron-scale intergranular pores between the brittle particles, such as those of quartz, pyrite, and clay minerals (Figure 7a,c). In addition, intergranular pores (measuring less than 1 μm) were frequently observed at the junction of pyrite particles (Figure 7d), and long interlaminar pores of clay minerals were seen to have easily formed between the flakey clay minerals and mixed illite-smectite (Figure 7c). The different types of minerals had evidently undergone phased dissolution phenomena with changes in the diagenetic fluid properties, and the round hole dissolution pores of the quartz and clay minerals in Well Yucan-6 were also seen to be developed (Figure 7b,f). Inorganic pores are mainly affected and controlled by compaction and diagenetic evolution, and they are often poorly connected and sorted.

Organic Pores

These are one of the key nanopore types found in shale, and their sizes range from several nanometers to hundreds of nanometers [37]. Organic matter pores are formed when OM undergoes thermal evolution, and such pores formed in the early stage of thermal evolution are usually either round or they have a honeycomb distribution (Figure 7e) with good connectivity, but they can also present as a long strip-shape due to the influence of late tectonic evolution. In the samples analyzed, there were more OM pores than inorganic pores, and the OM pore sizes were smaller with superior connectivity.

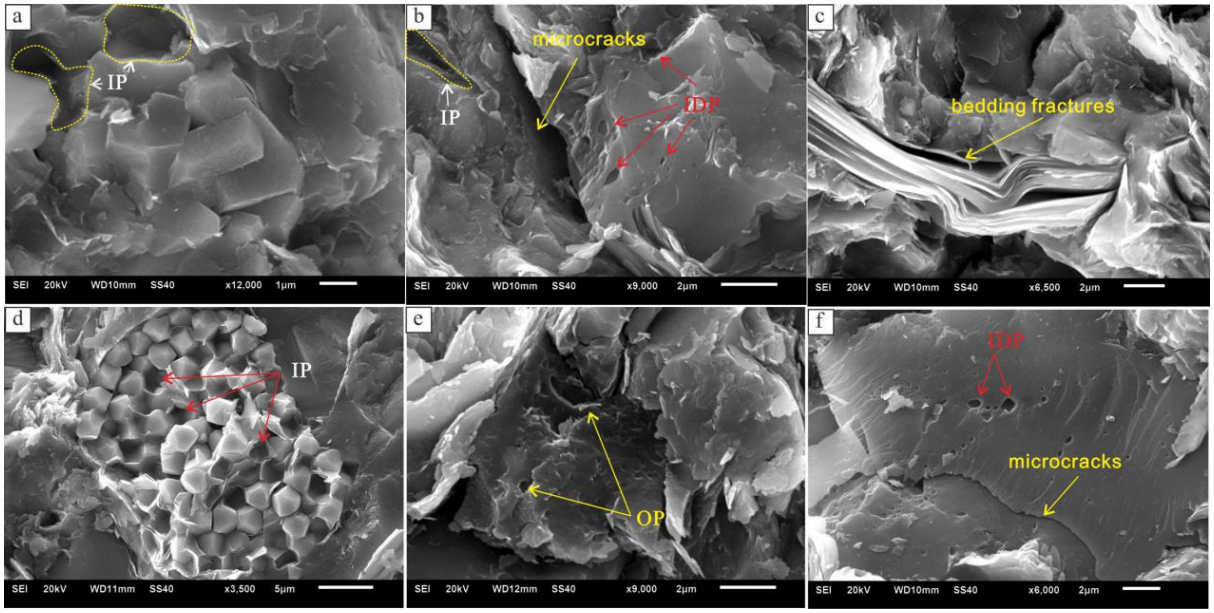

Figure 7. Microscopic characteristics of pores in shale reservoir of Well Yucan-6 (SEM). (**a**): Intergranular pores (IP) are distributed in pyrite within YC06-1 (Well Yucan-6) at 697.30 m; (**b**): Intragranular dissolved pores (IDP) existing in quartz grains, and intergranular pores and microcracks in YC06-6 (Well Yucan-6) at 708.71 m; (**c**): Bedding fractures of clay minerals in YC06-6 (Well Yucan-6) at 708.71 m; (**d**): Intergranular pore (IP) in Pyrite in YC06-19 (Well Yucan-6) at 722.53 m; (**e**): Organic pore (OP) in YC06-19 (Well Yucan-6) at 714.60 m; (**f**): Microcracks and intragranular dissolved pores (IDP) in YC06-41 (Well Yucan-6) at 744.50 m.

Micro Fractures

There are two micro fracture types: diagenetic fractures and structural fractures. Structural fractures often develop in jointed parts within strong structural areas when shale stress is released, such as in zones that contain both clay and brittle minerals (Figure 7b) or where irregular fractures exist (Figure 7f). Fracture strike is changeable and fractures are often later filled by calcite, quartz, and other veins; however, connectivity is usually poor. Diagenetic fractures are mainly affected by differential compaction and shrinkage caused by the diagenetic evolution of minerals and pore space changes. Shale easily forms as bedding interlayers in micro fractures (Figure 7c), and the existence of micro fractures is conducive for connecting isolated holes and promoting the permeability of shale pores.

5. Discussion

Shale gas exploration projects in South China have revealed obvious differences in the effects of shale development among the different layers within the Wufeng Longmaxi Formation [17,26]. This study conducted organic geochemical and reservoir characteristic analyses and identified a coupling relationship between the organic carbon content, OM maturity, mineral composition characteristics, pore size content, and adsorption capacity of shale in different layers of Well Yucan-6.

5.1. Relationship between OM Content and Mineral Composition

Shale is unlike other rock types in that it contains many clay minerals [29] that were mainly formed in a relatively deep-water sedimentary environment under a weak hydrodynamic force. A low-velocity water environment with a reduced terrestrial input is conducive for the formation of clay minerals and the enrichment and preservation of OM [27] In this respect, the sedimentary environment during the late Ordovician to Early Silurian in southern China was a deep-water shelf. This is reflected in the organic carbon content of the shale in the Wufeng-Longmaxi Formation within Well Yucan-6, which has a certain positive correlation with the clay minerals (Figure 8).

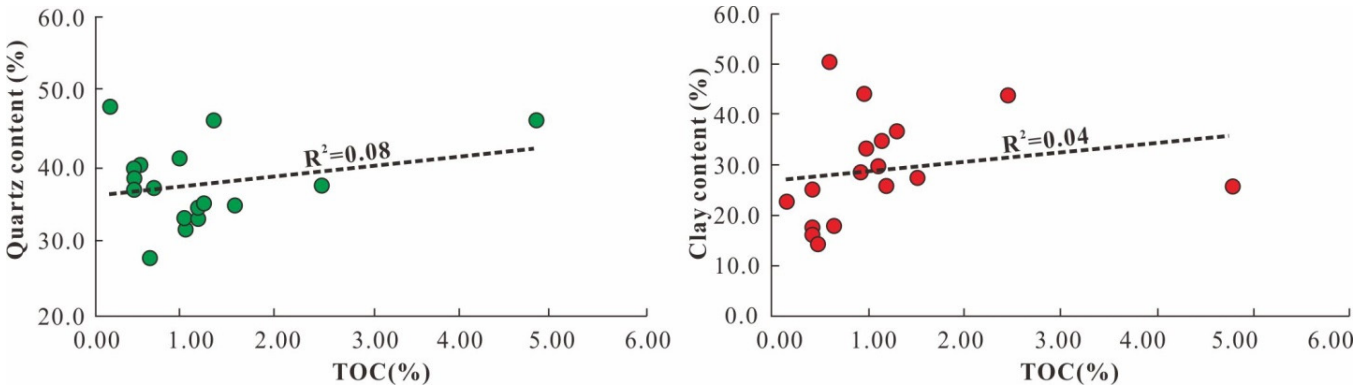

Figure 8. Relationship between TOC and mineral content within shale.

Some studies have found a positive correlation between the quartz and organic carbon contents of shale, which suggests that the many siliceous minerals present in the Wufeng-Longmaxi Formation shale in southern China were derived from biological sources [32,38]. Well Yucan-6 shows a positive correlation in this respect (Figure 8), but it has not yet been determined whether the early biogenic silica source promoted the enrichment of OM and increased the content of organic carbon within the shale. The SEM results show that the quartz is mainly terrigenous and authigenic, but only a small amount of biogenic quartz exists, an example of this being radiolarian. It is thus necessary to further investigate whether the silica source of these quartz is biogenic, or whether it is related to clay mineral transformation and release or diagenetic fluid filling.

5.2. Relationship between Mineral Composition and Reservoir Physical Properties

The clay and brittle mineral contents of shale are key factors that are analyzed during shale gas exploration and its later development. An appropriate mineral combination is necessary for the formation of a high quality organic shale reservoir, and it also provides a shale gas reservoir space with good shale gas and a strong adsorption capacity [21]. There is a positive correlation between the clay mineral content and porosity in the Wufeng-Longmaxi formation shale in Well Yucan-6, but a negative correlation between the brittle mineral content and porosity, which indicates that the shale pore space is mainly composed of nanopores. When the clay mineral content is high, the brittle mineral content is low, the isothermal adsorption capacity of the shale is large, and the existence of a large number of OM nanopores increases the overall shale porosity. (Figure 9). Furthermore, the existence of clay minerals provides a larger specific surface area for methane gas adsorption. Therefore, in terms of the shale reservoir space and adsorption capacity, a high clay mineral content implies the formation of a high-quality shale reservoir.

5.3. Relationship between TOC and Reservoir Physical Properties

To be identified as an oil and gas exploration target, shale needs to have a good hydrocarbon generation potential. The enrichment and hydrocarbon generation of OM in shale is related to the deposition of shale, late diagenesis, and tectonic evolution. During the thermal evolution process of OM, the formation of hydrocarbons creates a carbon phase change, which promotes the formation of shale nano pores [37]. In addition, the evolution of OM in the postmature stage can effectively promote the formation of a large number of nanopores in shale. With an increase in the TOC content [1,3], there is a gradual decrease in the pore size of the Wufeng-Longmaxi formation shale in Well Yucan-6, and an increase in its pore volume and porosity (Figure 10). This indicates that the enrichment of OM is beneficial for the existence of nanopores in the shale, and it plays an obvious role in porosity. At the same time, the isotherm adsorption capacity shows an obvious increasing trend with an increase in the TOC content (Figure 10), and this trend is stronger than the relationship between the clay mineral content and adsorbed gas content. This indicates

that the existence of OM provides a larger specific surface area for shale, which is key to promoting the shale adsorption capacity of natural gas.

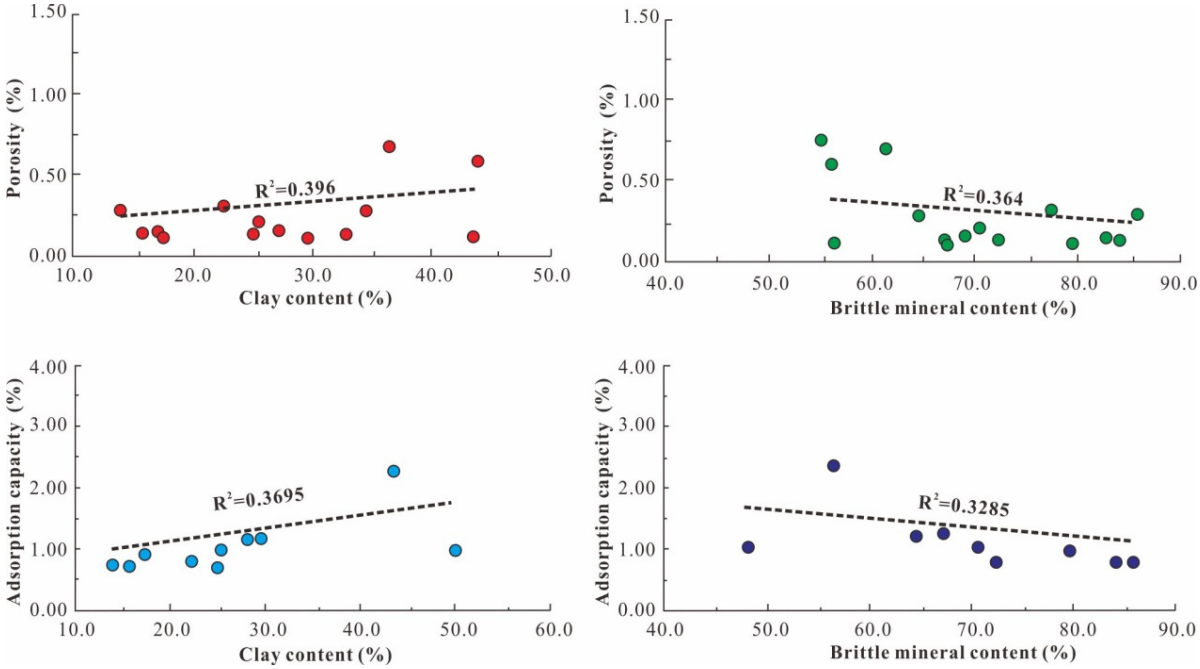

Figure 9. Relationship between mineral content, shale porosity, and adsorption capacity.

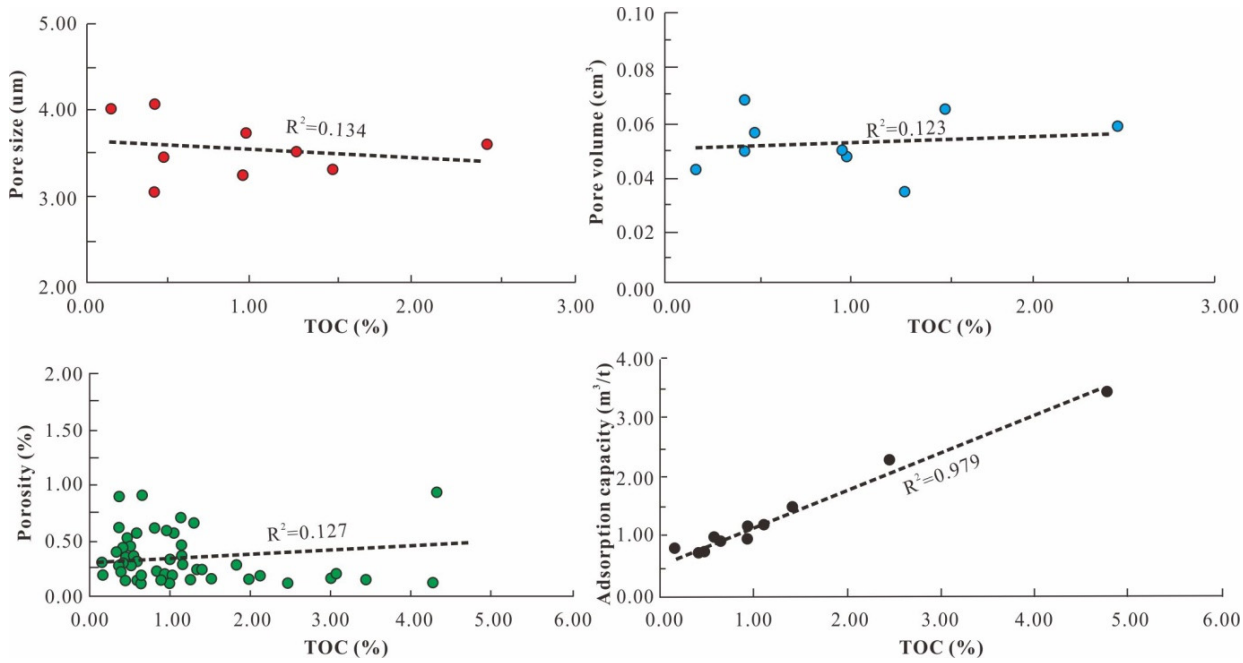

Figure 10. Relationship between TOC and reservoir physical parameters.

5.4. Coupling Characteristics

The results of this study have shown that the organic geochemistry of the Wufeng-Longmaxi shale has a complex coupling relationship with the reservoir characteristics (Figure 11). Differences in the mineral composition of shale not only affect the enrichment degree of organic carbon within it but also largely determine the pore structure and adsorption capacity of the shale. Shale with a high content of brittle minerals (such as quartz) generally have the following characteristics: developed inorganic pores, OM pores that are

not well developed, a relatively small specific surface area, and a weakened adsorption capacity. However, shale with a high clay mineral content promotes the development of organic pores, and the adsorption capacity increases with the increased specific surface area. In relation to the particular geological background of southern China, the shale is generally characterized as having high OM abundance, and it has undergone strong structural transformations [8,26]. To compensate for the influence of tectonic damage during later stage development, high-quality shale reservoirs need to have a strong adsorption capacity and a large number of nanopores to preserve the natural gas within the shale, and the desorption process can then be completed after fracturing.

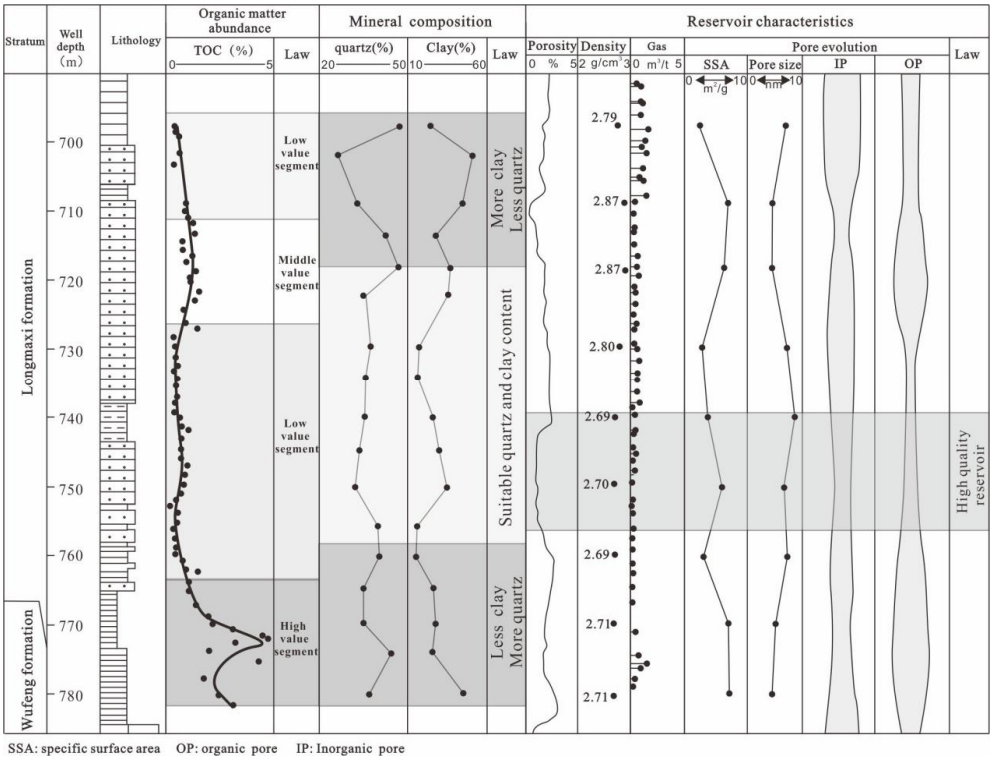

Figure 11. Coupling relationship between shale organic geochemistry and reservoir characteristics of Well Yucan-6.

5.5. Revelations of Shale Gas Exploration

The organic geochemical indicators of the Wufeng-Longmaxi shale in southern China are generally good; however, the multiple hydrocarbon generation and expulsion processes of OM and the late structural damage are likely to have restricted shale gas accumulation [8,26]. Developing measures to reduce the loss of natural gas in shale becomes particularly important. At present, reservoirs that have undergone stable tectonic evolution and which have good preservation conditions are selected for shale gas exploration and development [8,18]. However, the adsorption characteristics of shale can overcome or weaken the migration and loss of natural gas; therefore, shale layers that have a strong adsorption capacity are likely to develop shale gas in favorable reservoir forming areas. The coupling relationship between organic geochemistry and the reservoir of shale in Well Yucan-6 indicates that it has a high clay mineral content and TOC content with a strong adsorption capacity and a large number of nanopores. It is therefore considered feasible that shale gas fracturing development could be conducted on shale layers that have a high TOC content, high clay mineral content, and an appropriate quartz content.

6. Conclusions

Through the above research, the following points were proved. At the bottom of the Wufeng-Longmaxi Formation in Well Yucan-6, the average TOC content of the shale is

3.04%; this value gradually decreases upwards, and the average value throughout the entire section is 0.78%. The OM type is mainly kerogen I, the average Ro value is 1.94%, the OM is in a postmature thermal evolutionary stage, and all of the organic geochemical indicators indicate that the source rock is of a good quality; the Wufeng-Longmaxi Formation shale reservoir in Well Yucan-6 has low porosity and permeability, and it is mainly composed of quartz and clay minerals with various pore types (including intergranular pores, intragranular dissolved pores, organic matter pores, and micro fractures); clay-rich mineral shale usually has a high OM content when formed in a deep-water sedimentary environment, and the clay minerals are not only conducive to the formation of nano pores in shale, but they also expand the specific surface area of shale. Organic matter forms a large number of OM nanopores during the process of high thermal evolution, and this enhances the shale adsorption ability. Based on the coupling relationship determined in this study between the geochemistry and reservoir characteristics, it was determined that the most favorable horizon for shale gas development in the Wufeng-Longmaxi Formation of Well Yucan-6 is the shale section with a high clay content, high TOC value, and an optimum quartz content.

Author Contributions: Funding acquisition, D.L.; Investigation, X.Z.; Methodology, Y.Z.; Project administration, W.J. and J.W. (Jinxi Wang); Resources, Z.L.; Software, Z.Y.; Writing—original draft, S.W.; Writing—review & editing, J.W. (Jia Wang) and X.T. All authors have read and agreed to the published version of the manuscript.

Funding: This research was funded by the National Natural Science Foundation of China, Grant Numbers 41902153 and 41672113, and the Natural Science Foundation Project of CQ CSTC, Grant Numbers cstc2018jcyjAX0523 and cstc2020jcyj-msxm0778.

Institutional Review Board Statement: Not applicable.

Informed Consent Statement: Not applicable.

Data Availability Statement: Not applicable.

Acknowledgments: We greatly thank the Chongqing Municipal Bureau of Planning and Natural Resources for the implementation and affirmation of Well Yucan-6, as well as all the staff of Chongqing Institute of Geology and Mineral Resources for participating in drilling and analysis of Well Yucan-6. We thank our scientific research team for their help and guidance in the field investigation.

Conflicts of Interest: The authors declare no conflict of interest.

References

1. Loucks, R.G.; Reed, R.M.; Rrppel, S.C.; Hammes, U. Spectrum of pore types and networks in mud rocks and descriptive classification for matrix-related mud rocks pore. *AAPG Bull.* **2012**, *96*, 1071–1098. [CrossRef]
2. Loucks, R.; Ruppel, S. Mississippian Barnett shale: Lithofa-cies and depositional setting of a deep-water shale-gas succession in the Fort Worth basin, Texa. *AAPG Bull.* **2007**, *91*, 579–601. [CrossRef]
3. Curtis, M.E.; Cardott, B.; Sondergeld, C.H.; Rai, C.S. Development of organic porosity in the Woodford Shale with increasing thermal maturity. *Int. J. Coal Geol.* **2012**, *103*, 26–31. [CrossRef]
4. Ross, D.J.; Bustin, R. Characterizing the shale gas resource potential of Devonian-Mississippian strata in the Western Canada sedimentary basin: Application of an integrated formation evaluation. *AAPG Bull.* **2008**, *92*, 87–125. [CrossRef]
5. Jinchuan, Z.; Xu, B.; Haikuan, N.; Zongyu, W.; Lin, T. Exploration potential of shale gas resources in China. *Nat. Gas Ind.* **2008**, *28*, 136–140.
6. Caineng, Z.; Songqi, P.; Qun, Z. On the connotation, challenge and significance of China's "energy independence" strategy. *Pet. Explor. Dev.* **2020**, *47*, 416–426.
7. Xusheng, G. Controlling factors on shale gas accumulations of Wufeng-Longmaxi Formations in Pingqiao shale gas field in Fuling area, Sichuan Basin. *Nat. Gas Geosci.* **2019**, *30*, 1–10.
8. Zhenxue, J.; Yan, S.; Xianglu, T.; Zhao, L.; Xingmeng, W.; Guozhen, W.; Zixin, X.; Xin, L.; Kun, Z.; Jiaqin, C.; et al. Controlling factors of marine shale gas differential enrichment in southern China. *Pet. Explor. Dev.* **2020**, *47*, 617–628.
9. Jinlei, L.; Cheng, Y.; Mingfei, W.; Shasha, Y.; Xiaojing, L.; Chao, C. Preservation condition differences in Jiaoshiba area, Fuling, Sichuan Basin. *Petrol. Geol. Exper.* **2019**, *41*, 341–347.

10. Zhen, Q.; Caineng, Z.; Hongyan, W.; Dazhong, D.; Bin, L.; Zhenhong, C.; Dexun, L.; Guizhong, L.; Hanlin, L.; Jianglin, H.; et al. Discussion on characteristics and controlling factors of differential enrichment of Wufeng-Longmaxi formations shale gas in South China. *J. Nat. Gas. Geosci.* **2020**, *5*, 117–128.
11. Chenglin, Z.; Jian, Z.; Wuguang, L.; Chong, T.; Chao, L.; Shengxian, Z.; Wenwen, Z. Deep shale reservoir characteristics and exploration potential of Wufeng-Longmaxi Formations in Dazu area, western Chongqing. *Nat. Gas. Geosci.* **2019**, *30*, 1794–1804.
12. Gomaa, S.; Emara, R.; Mahmoud, O.; El-Hoshoudy, A.N. New correlations to calculate vertical sweep efficiency in oil reservoirs using nonlinear multiple regression and artificial neural network. *J. King Saud Univ.-Eng. Sci.* **2021**, in press. [CrossRef]
13. Adegbite, J.O.; Belhaj, H.; Bera, A. Investigations on the relationship among the porosity, permeability and pore throat size of transition zone samples in carbonate reservoirs using multiple regression analysis, artificial neural network and adaptive neuro-fuzzy interface system. *Pet. Res.* **2021**, in press. [CrossRef]
14. Ghareb, H.; Veronique, J. Developed correlations between sound wave velocity and porosity, permeability and mechanical properties of sandstone core samples. *Pet. Res.* **2020**, *5*, 326–338.
15. Powley, D. Pressures and hydrogeology in petroleum basins. *Earth Sci. Rev.* **1990**, *29*, 215–226. [CrossRef]
16. Yassin, M.; Begum, M.; Dehgahnpour, H. Organic shale wettability and its relationship to other petrophysical properties: A Duvernay case study. *Int. J. Coal Geol.* **2017**, *169*, 74–91. [CrossRef]
17. Tonglou, G. Key geological issues and main controls on accumulation and enrichment of Chinese shale gas. *Pet. Explor. Dev.* **2016**, *43*, 317–326.
18. Tonglou, G.; Ruobing, L. Implications from marine shale gas exploration breakthrough in complicated structural area at high thermal stage: Taking Longmaxi formation in Well JY1 as an example. *Nat. Gas Geosci.* **2013**, *24*, 643–651.
19. Tonglou, G.; Hanrong, Z. Formation and enrichment mode of Jiaoshiba shale gas field, Sichuan Basin. *Pet. Explor. Dev.* **2014**, *41*, 31–40.
20. Martineau, D. History of the Newark East field and the Barnett Shale as a gas reservoir. *AAPG Bull.* **2007**, *91*, 399–403. [CrossRef]
21. Caieng, Z.; Zhi, Y.; Shizhen, T.; Wei, L.; Songtao, W.; Rukai, Z.; Xuanjun, Y.; Lan, W.; Xiaohui, G.; Jinhua, J.; et al. Nano-hydrocarbon and the accumulation in coexisting source and reservoir. *Pet. Explor. Dev.* **2012**, *39*, 15–32.
22. Thanh, H.V.; Sugai, Y.C.; Sasaki, K. Impact of a new geological modelling method on the enhancement of the CO_2 storage assessment of E sequence of Nam Vang field, offshore Vietnam. *Energy Sources* **2020**, *42*, 1499–1512. [CrossRef]
23. Jia, W.; Xianfeng, T.; Jingchuan, T.; Long, L.; Xuanbo, G.; Chao, L.; Chunlin, Z.; Lei, Z.; Weiwei, X. The Effect of Diagenetic Evolution on Shale Gas Exploration and Development of the Longmaxi Formation Shale, Sichuan Basin, China. *Front. Earth Sci.* **2021**, *9*, 172. [CrossRef]
24. Thanh, H.V.; Sugai, Y.C. Integrated modelling framework for enhancement history matching in fluvial channel sandstone reservoirs. *Upstr. Oil Gas Technol.* **2021**, in press. [CrossRef]
25. Zhuo, L.; Zhenxue, J.; Xianglu, T.; Pengfei, W.; Pu, H.; Guozhen, W. Lithofacies Characteristics and Its Effect on Pore Structure of the Marine Shale in the Low Silurian Longmaxi Formation, Southeastern Chongqing. *Earth Sci.* **2017**, *42*, 1116–1123.
26. Jia, W.; Xianfeng, T.; Jingchun, T.; Chao, L.; Tian, R.; Qing, C.; Xia, L.; Chunlin, Z. Constraints of hydrocarbon migration in Longmaxi shale in Sichuan Basin on shale gas accumulation. *Pet. Geol. Exp.* **2017**, *39*, 755–762.
27. Chuanlong, M.; Xiangying, G.; Xiaosong, X.; Kenken, Z.; Wei, L.; Xiuping, W. Lithofacies palaeogeography of the Late Ordovician and its petroleum geological significance in Middle-Upper Yangtze region. *J. Palaeogeoraphy* **2014**, *16*, 427–440.
28. Xusheng, G.; Yuping, L.; Tenger, B.; Qiang, W.; Tao, Y.; Baojian, S.; Zhongliang, M.; Fulbin, W. Hydrocarbon generation and storage mechanisms of deep-water shelf shales of Hydrocarbon generation and storage mechanisms of deep-water shelf shales of, China. *Pet. Geol. Exp.* **2020**, *47*, 193–201.
29. Digang, L.; Tonglou, G.; Jianping, C.; Lizeng, B.; Zhe, Z. Distribution of four suits of regional marine source rocks, South China. *Mar. Orig. Pet. Geol.* **2008**, *13*, 1–16.
30. Peters, K.; Cassa, M. Applied source rock geochemistry. *AAPG Bull.* **1994**, *60*, 93–120.
31. Jacob, H. Dispersed solid bitumens as an indicator for migration and maturity in prospecting for oil and gas. *Erdöl Kohle Erdgas Petrochem.* **1985**, *38*, 365–392.
32. Xiuping, W.; Chuanlong, M.; Qiyu, W.; Xiangying, G.; Xiaowei, C.; Kenken, Z.; Wei, L. Diagenesis of black shale in Longmaxi Formation, southern Sichuan Basin and its periphery. *Acta Petrol. Sin.* **2015**, *36*, 1035–1047.
33. Shugen, L.; Zhiwu, L.; Wei, S.; Zhili, L.; Guozhi, W.; Zhiquan, Y.; Wenming, H. Basic geological features of superimposed baisn and hydrocarbon accumulatuion in Sichuan Basin, China. *Chin. J. Geol.* **2011**, *46*, 233–257.
34. Caineng, Z.; Rukai, Z.; Bin, B.; Zhi, Y.; Songtao, W.; Ling, S.; Dazhong, D.; Xingjing, L. First discovery of nano-pore throat in oil and gas reservoir in China and its scientific value. *Acta Petrol. Sin.* **2011**, *277*, 1857–1864.
35. Haihan, Q.; Yuping, Z.; Ye, Y. An analysis on "double hump distribution of intrusive" mercury curve. *Acta Petrol. Sin.* **1999**, *20*, 61–68.
36. Sing, K.S.W.; Everett, D.H.; Haul, R.A.W.; Moscou, L.; Pierotti, R.A.; Rouquerol, J.; Siemieniewska, T. Reporting phys-isorption data for gas/solid with special reference to the determination of surface systems area and porosity. *Pure Appl. Chem.* **1985**, *57*, 603–619. [CrossRef]
37. Jarvie, D. Unconventional shale resource plays: Shale gas shale oil opportunities. *Tex. Word-Wide Geochem.* **2008**, 7–17. Available online: https://www.yumpu.com/en/document/view/10690125/unconventional-shale-resource-plays-shale-gas-and-shale-oil (accessed on 5 September 2021).
38. Shufang, W.; Caineng, Z.; Dazhong, D.; Yuman, W.; Jinliang, H.; Zhaojie, G. Biogenic silica of organic-rich shale in Sichuan Basin and Its significance for shale gas. *Acta Sci. Nat. Univ. Pekin.* **2014**, *50*, 476–486.